# A first-principles study on new high-pressure metastable polymorphs of MoO$_2$

Nils Becker [a], Richard Dronskowski [a,b,*]

[a] Institut für Anorganische Chemie, RWTH Aachen University, Landoltweg 1, D-52056 Aachen, Germany
[b] Jülich-Aachen Research Alliance (JARA-HPC), RWTH Aachen University, D-52074 Aachen, Germany

## ARTICLE INFO

## ABSTRACT

The pressure-dependence of the stabilities of several MoO$_2$ phases has been investigated by density-functional theory (GGA/PBE/PAW). Out of a set of 15 MX$_2$ structures, the [SnO$_2$(II)], [$\alpha$-PbO$_2$], and a modified rutile structure type were identified as possible metastable MoO$_2$ polymorphs based on the analysis of thermodynamic properties and dynamic stability. High-pressure calculations suggest an orthorhombic TiO$_2$ structure, dubbed [*ortho*-TiO$_2$], as a high-pressure polymorph at around 25 GPa. Furthermore, we find that the previously reported rutile-type MoO$_2$ may be understood as a modified rutile type similar to the [VO$_2$] structure.

© 2016 Elsevier Inc. All rights reserved.

## 1. Introduction

There are only two binary oxides with simple oxidation states ($+$VI,$+$IV) known for molybdenum, namely MoO$_3$ and MoO$_2$. The latter, molybdenum dioxide, is a brown-purple solid obtained through reduction of molybdenum trioxide using hydrogen at temperatures below 743 K [1]. The first complete crystal-structure analysis was performed by Brandt and Skapski in 1967 [2]. In nature, the phase can be found as the rare mineral Tugarinovite. MoO$_2$ shows a metal-like electrical conductivity which is unusual among other transition-metal oxides [3,4]. Technological applications of the dioxide are not as widespread as for MoO$_3$ but include the selective oxidation catalysis of various organic compounds [5–8] and, also, a promising anode material for lithium-ion batteries [4,9–11]. Recent interest in MoO$_2$ emerged from applications as films for energy storage [12,13] and as a soft-magnetic and optical material [14–16]. Nanorods of MoO$_2$ have also been reported [17]. Previous quantum-theoretical studies on MoO$_2$ include tight-binding approaches [18], cluster calculations [19–22], a study of the Peierls-like instability in MoO$_2$ using LDA-ASW [23] and a GGA-based analysis of the electronic structure of MoO$_2$ [24]. The work by Eyert et al. [23] includes a detailed analysis of the electronic structure of monoclinic MoO$_2$ and the (hypothetical) rutile MoO$_2$ which leads to the conclusion that the monoclinic

structure is a result of a Peierls-type instability of the rutile structure. The GGA-based work by Scanlon et al. [24] focuses on the (electronic) structure of MoO$_2$ (and MoO$_3$) and arrives at a good agreement between the theoretical calculations and previous experimental results.

MoO$_2$ crystallizes in a rutile-type structure distorted in such a way that the molybdenum atoms form Mo–Mo dumbbells with alternating bond lengths of about 2.51 Å and 3.02 Å, the aforementioned Peierls scenario. This is the only widely known polymorph of MoO$_2$. Another tetragonal rutile-type form initially reported by Goldschmidt et al. in 1926 [25] has only been re-reported once, in 2004 [26], but it has not been confirmed by other sources ever since. Here we present a first-principles approach to the MoO$_2$ system in the search for metastable polymorphs, to be synthesized at elevated temperatures or pressures including the proposal of its possible synthetic conditions.

## 2. Theoretical methods

Periodic density-functional theory (DFT) calculations were performed as implemented in the Vienna ab initio simulation package (VASP) [27]. Core and valence electrons were separated using projector-augmented waves (PAW) [28], and the generalized-gradient-approximation as described by Perdew et al. (GGA-PBE) [29,30] was used to treat contributions of exchange and correlation. Owing to the layered nature of some investigated MX$_2$

* Corresponding author at: Institut für Anorganische Chemie, RWTH Aachen University, Landoltweg 1, D-52056 Aachen, Germany.

structure types, additional corrections for van-der-Waals forces had to be included, namely Grimme's "D3(BJ)" dispersion correction with Becke–Johnson damping [31,32] as implemented in VASP 5.3.5. An energy-cutoff of 500 eV and an adapted $k$-point sampling ensured well-converged structures. All lattice parameters and atomic positions were allowed to relax until the ionic convergence criterion of $10^{-6}$ eV was reached. A set of 15 $MX_2$ structures featuring mostly sixfold coordination (and eightfold [$CaF_2$] and [$ZrO_2$], because of the tendency of high-pressure phases for larger coordination numbers) of the metal atom was chosen as a starting point for the investigation, followed by full-structural relaxation to find the lowest-energy structures.

In order to predict high-pressure polymorphs the structural volumes were varied by scaling the cell parameters from 94% to 104%, and the resulting energy vs. volume data were fitted to the Birch–Murnaghan equation of state [33]. Thus, the pressure and, eventually, the reaction enthalpies as a function of the pressure were calculated.

The thermodynamic properties of selected $MO_2$ candidates were calculated using the program Phonopy [34]. As a first step, supercells of the optimized structures were constructed. All symmetry-inequivalent atoms were then slightly shifted out of their equilibrium positions to calculate the Hellmann–Feynman forces. Subsequently, the force constants and then the dynamical matrices were computed. Through combination of the eigenvalues (phonon frequencies) with Bose–Einstein statistics, the free phonon energy was obtained [35]. The thermodynamic properties at finite temperatures are straightforwardly accessible from these theoretical data.

## 3. Results and discussion

As said before, the only widely known polymorph of $MoO_2$ crystallizes in the monoclinic [$VO_2$] type (space group $P2_1/c$) with the lattice parameters $a = 5.6109$ Å, $b = 4.8562$ Å, $c = 5.6285$ Å together with a monoclinic angle of 120.95° [2]. The crystal structure is a rutile type distorted to a monoclinic supercell containing four $MoO_2$ formula units. The rutile $c$ axis can be found in the $ac$ layer of the [$VO_2$] structure [24]. From now on we will designate this experimentally known phase as $\alpha$-$MoO_2$. A true rutile-type polymorph of $MoO_2$ has only been reported twice [25,26], first in 1926, then in 2004, as said before.

A set of 15 $MX_2$ structures was selected to investigate the $MoO_2$ system for new metastable or high-pressure polymorphs. Just like the experimentally known [$VO_2$] structure of $\alpha$-$MoO_2$, the 14 other investigated structures also feature at least sixfold coordination ($CaF_2$ and $ZrO_2$: eightfold coordination) for the molybdenum atom, mostly a distorted octahedron. As molybdenum dioxide crystallizes in a distorted rutile structure, focusing on similar structures seems rather straightforward although radically different structural candidates (possibly accessible by evolutionary algorithms) may go unnoticed.

The selected structures were structurally optimized for the composition $MoO_2$ using the GGA-PBE functional. Contributions of van-der-Waals forces were included using "D3(BJ)" dispersion correction to properly describe layered structures such as [$\alpha$-$MoS_2$]. The structural parameters calculated by the GGA approach for $\alpha$-$MoO_2$ are in excellent agreement with the experimental observation (Table 1) as well as previous GGA calculations [24] with respect to the atomic positions and only show the rather typical but small GGA D3(BJ) overestimation of the lattice parameter. The calculated electronic DOS is also in good agreement with previous experimental [23] and theoretical [24] work. All electronic DOS are provided in the SI.

The calculated energies and volumes of all optimized $MX_2$ structures are listed in Table 2. The energetically favored structure,

**Table 1**

Structural data (Å,°) of the optimized [$VO_2$] structure of $MoO_2$ (space group $P2_1/c$, $Z=4$) employing the GGA-PBE potential including D3-correction compared to experimental results (italics) from the literature [2].

|  |  | Atom | Wyck. | $x$ | $y$ | $z$ |
|---|---|---|---|---|---|---|
| $a$ | 5.590 | Mo1 | 4$e$ | 0.231 | 0.992 | 0.017 |
|  | *5.6109(8)* |  |  | *0.2316* | *0.9916* | *0.0164* |
| $b$ | 4.904 | O1 | 4$e$ | 0.113 | 0.217 | 0.235 |
|  | *4.8562(6)* |  |  | *0.112* | *0.217* | *0.233* |
| $c$ | 5.665 | O2 | 4$e$ | 0.390 | 0.697 | 0.298 |
|  | *5.6285(7)* |  |  | *0.391* | *0.697* | *0.298* |
| $\beta$ | 120.72 |  |  |  |  |  |
|  | *120.95(1)* |  |  |  |  |  |
| $V$ | 133.49 Å$^3$ |  |  |  |  |  |
|  | *131.53 Å$^3$* |  |  |  |  |  |

**Table 2**

Calculated relative energies, total volumes per $MoO_2$ formula unit and bulk moduli as a function of the starting structure types.

| Starting structure | $\Delta E$ (eV) | $V$ (Å$^3$) | $B_0$ (GPa) | Reference |
|---|---|---|---|---|
| [$VO_2$] | 0 | 33.38 | 232 | [2] |
| [$SnO_2$(II)] | 0.105 | 33.20 | 234 | [36] |
| [$\alpha$-$PbO_2$] | 0.122 | 32.83 | 222 | [44] |
| [$\alpha$-$MoS_2$] | 0.151 | 34.12 | 49 | [44] |
| [$\beta$-$MoS_2$] | 0.153 | 34.27 | 50 | [44] |
| [$CaCl_2$] | 0.176 | 33.28 | 276 | [44] |
| [$TiO_2$] (rutile) | 0.176 | 33.26 | 278 | [44] |
| Brookite | 0.283 | 33.03 | 184 | [45] |
| Anatase | 0.501 | 32.43 | 179 | [44] |
| [$ortho$-$TiO_2$] | 0.548 | 29.19 | 259 | [42] |
| [$VO_2$(B)] | 0.615 | 38.76 | 182 | [46] |
| [$ZrO_2$] (Baddeleyite) | 0.791 | 30.80 | 204 | [47] |
| [$FeS_2$] | 1.001 | 30.90 | 283 | [48] |
| [$CaF_2$] | 1.127 | 29.48 | 299 | [44] |
| Cotunnite | 1.183 | 29.39 | 141 | [49] |

as expected, is the experimental [$VO_2$] ground state which immediately gets corroborated. Additionally, the [$CaCl_2$] structure, a distorted rutile type, transforms into the rutile type [$TiO_2$] upon structural optimization. Furthermore, there are five structure types that are at most 0.2 eV (19 kJ/mol) less stable than [$VO_2$]. These are [$SnO_2$(II)], [$\alpha$-$PbO_2$], [$\alpha$-$MoS_2$], [$\beta$-$MoS_2$], and [$TiO_2$], and they represent possible metastable polymorphs of $MoO_2$ as they are energetically only slightly less favored. All other structure types are less stable by at least 27–50 kJ/mol than the experimental polymorph. Because such large energy barriers are very unlikely to be overcome, these structures were not investigated any further.

The [$SnO_2$(II)] structure type is a high-pressure polymorph of $SnO_2$ crystallizing in the orthorhombic space group *Pbcn* (No. 60) where the metal atoms are octahedrally coordinated by O atoms. The octahedra are slightly distorted and connected to each other using only 1/6th of all edges [36]. Compared to the (ideal) rutile structure showing linear chains of edge-connected octahedra, those in the $SnO_2$(II) structure are tilted by 108.5° after every fourth octahedron (see Fig. 1, left). The chains are corner-connected in the $a$ direction but unconnected along $b$.

Scrutinyite is the natural $PbO_2$ mineral that crystallizes in the orthorhombic $\alpha$-$PbO_2$ structure with space group *Pbcn* (No. 60). It can be described as a slightly distorted hcp of oxygen atoms with the metal atoms occupying half of the octahedral interstitial sites. The $PbO_2$ (or $MoO_2$) octahedra form edge-connected zigzag chains along the $c$ axis and alternating layers along the $a$ direction (Fig. 1, center). Furthermore, the chains are corner-connected along $a$.

The well-known crystal structure of the mineral Molybdenite ($\beta$-$MoS_2$) can be described as a layered structure based on hexagonal close-packed layers of sulfur atoms incorporating the molybdenum atoms. The trigonal prismatic coordination spheres with
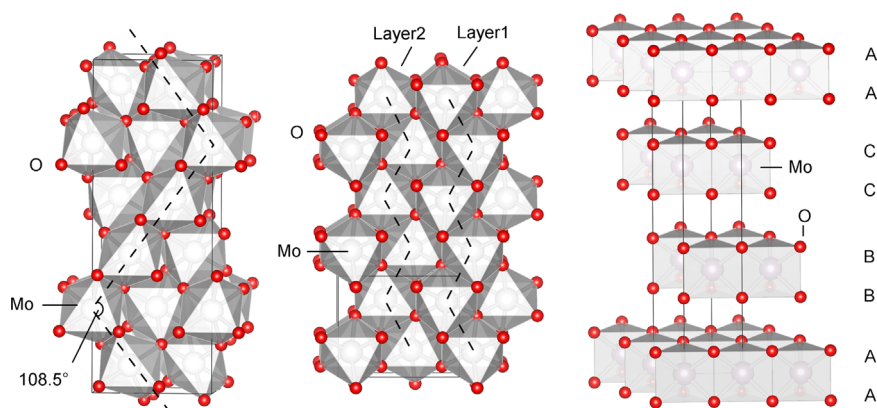
**Fig. 1.** Crystal structures of the three calculated polymorphs of MoO$_2$ displaying the lowest energy compared to [VO$_2$]: SnO$_2$(II) (left), $\alpha$-PbO$_2$ (center) and $\alpha$-MoS$_2$ (right).

the sulfur atoms on their vertices are half-occupied by the molybdenum atoms within each layer. The unit cell of [$\beta$-MoS$_2$] consists of two of these described "sandwich" layers (S-Mo-S) that are shifted, resulting in a [AABB] layer sequence. [$\alpha$-MoS$_2$] (Fig. 1, right) differs from the $\beta$-phase only in the varying layer sequence [AABBCCAA].

Aside from the two [MoS$_2$] structure types all other possible polymorphs show an octahedral coordination of the molybdenum atoms by oxygen atoms, as said before, and are more or less closely related to the rutile structure type.

In order to further narrow down the set of possible polymorphs, the dynamic stability of these five phases ($\Delta E < 0.2$ eV) was compared by calculating the phonon DOS at ambient pressure as shown in Fig. 2. Surprisingly, the rutile structure exhibits a considerable amount of imaginary modes and is therefore dynamically unstable. This makes a metastable polymorph of MoO$_2$

with a rutile structure unlikely such that the experimental result by Seisenbaeva et al. [26] seems to question the theoretical one. A detailed look at the calculated imaginary modes (see below) might shed some light on this discrepancy between experimental observation and theoretical calculation. The imaginary modes found for [$\alpha$-PbO$_2$] are fairly small, however, so further investigations will be needed to clarify its (meta-)stability. For the remaining structures [VO$_2$], [SnO$_2$(II)] and both [MoS$_2$] types, the calculated phonon DOS do not show any imaginary modes and therefore prove their dynamic stability.

As mentioned above, MoO$_2$ is dynamically unstable in the rutile-type structure. To investigate the source of the instability and hopefully find a stable modification, the structure was modified by shifting the atoms along eigenvectors that were created in the process of the phonon calculation. The resulting structure was then once again allowed to fully relax. During the process the
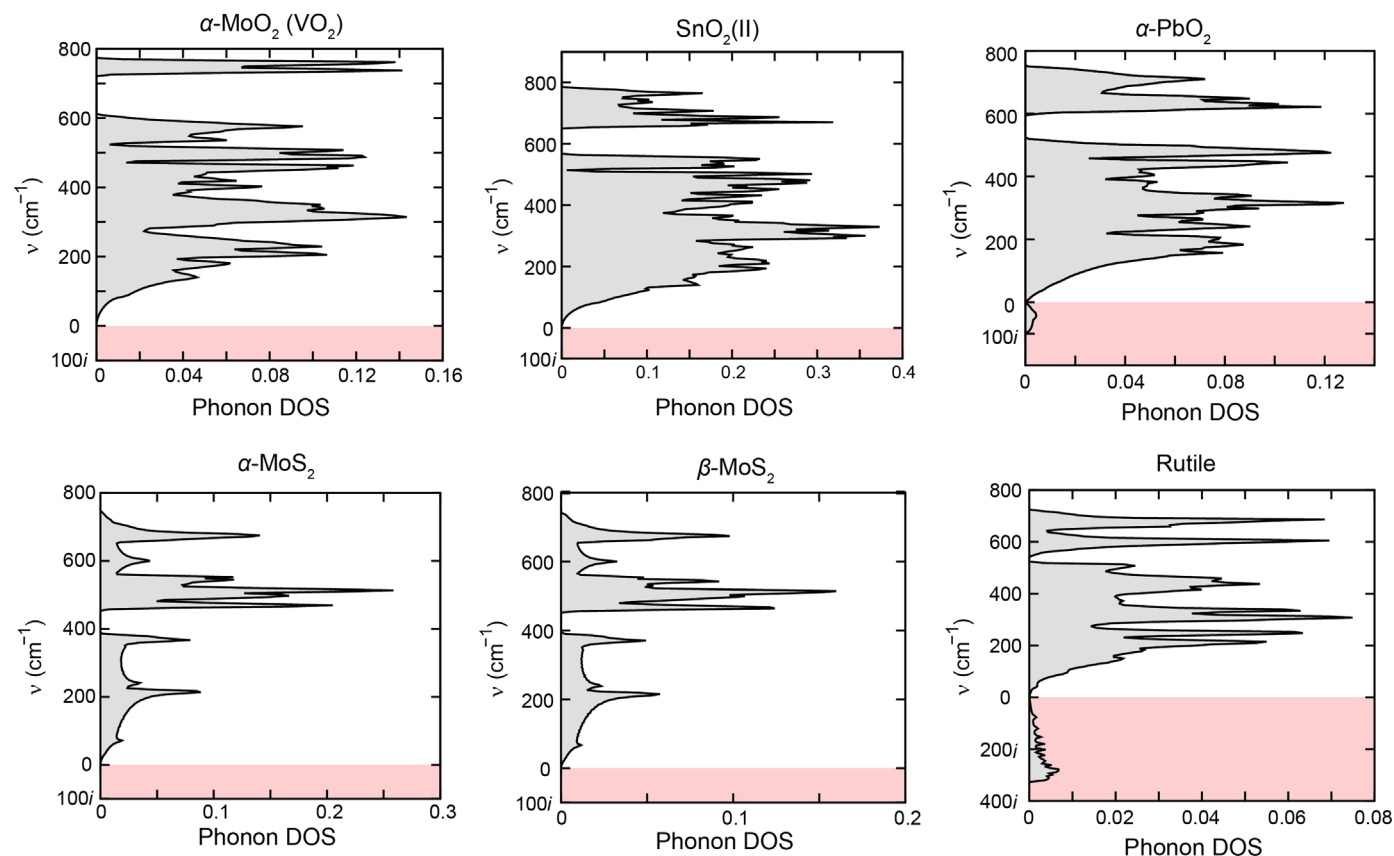


**Fig. 2.** Calculated phonon density of states of the energetically most favorable structure types for MoO$_2$ at ambient pressure.
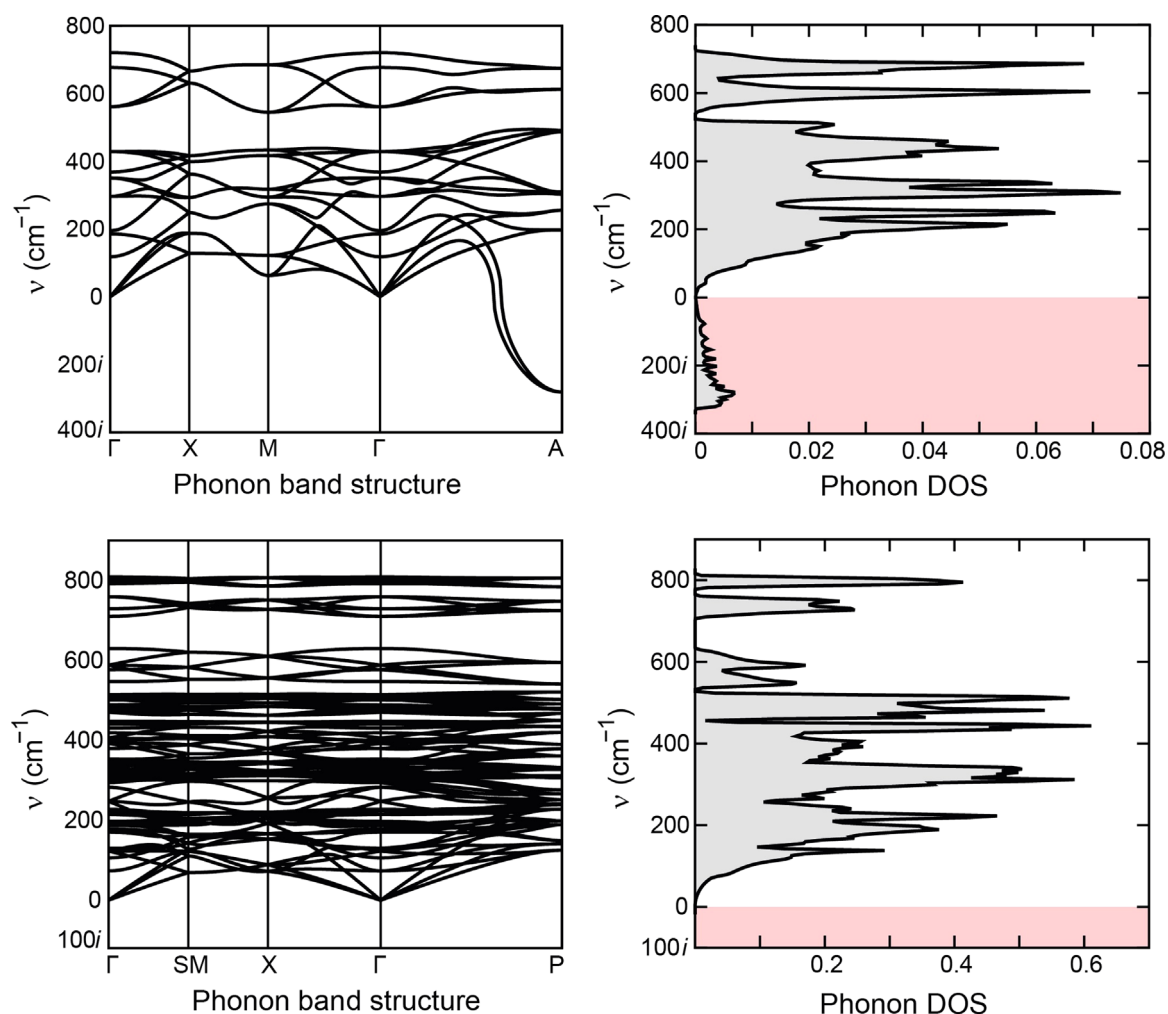
**Fig. 3.** Calculated phonon band structure and DOS of $MoO_2$ in the rutile structure (top) and distorted rutile structure (bottom).

space group lowered from $P4_2/mnm$ (136) to $I4_1md$ (109). This structure will now be referred to as a "modified" rutile type [mod–$TiO_2$].

$MoO_2$ in the modified rutile-type is 0.09 eV per formula unit more stable than in the original rutile type and only 0.08 eV per formula unit (8 kJ/mol) less stable than monoclinic $\alpha$-$MoO_2$. Phonon calculations of this modified rutile structure were performed to test its dynamic stability. The corresponding new phonon band structure and phonon DOS presented in Fig. 3 (bottom) show no imaginary modes and thus demonstrates the dynamic stability of the modified rutile structure. A dynamically stable structure with

such a small energy difference to the stable polymorph is an excellent candidate for a metastable polymorph. In contrast, the attempt to find a dynamically stable structure of $\alpha$-$PbO_2$ in an analogous way did not succeed. Nonetheless, the past has shown that a synthesis can be successful even when the calculated phonon band structure is unfavorable: $\gamma$-TaON, for example, has recently been synthesized although its pDOS exhibits imaginary frequencies [35,37].

When comparing the structure of $\alpha$-$MoO_2$, the original [$VO_2$] type, with the modified rutile structure (see Fig. 4) both structures look very similar. Both feature two distinct short Mo–Mo distances
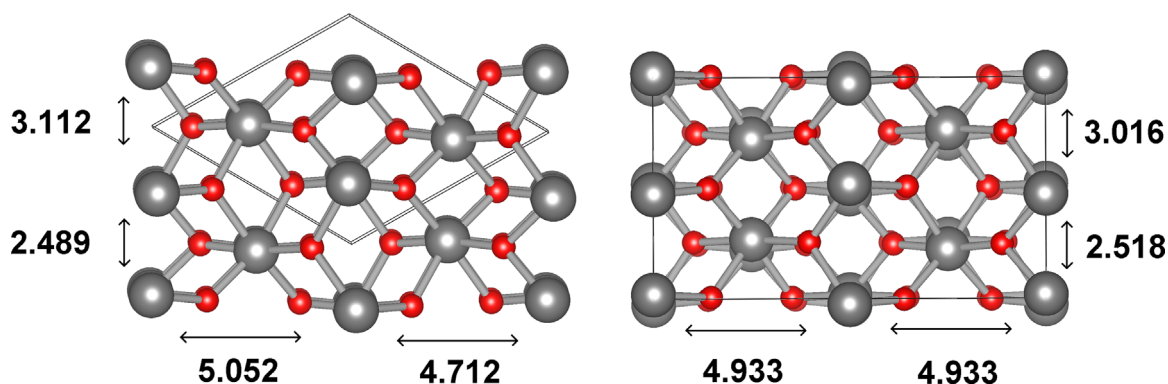


**Fig. 4.** Unit cell of the modified rutile structure (right) compared to the equivalent sized super cell [$VO_2$] structure (left) of $MoO_2$ with the unit cell shown. Displayed are the Mo–Mo distances (Å) along the rutile $a$ and $c$ axes.
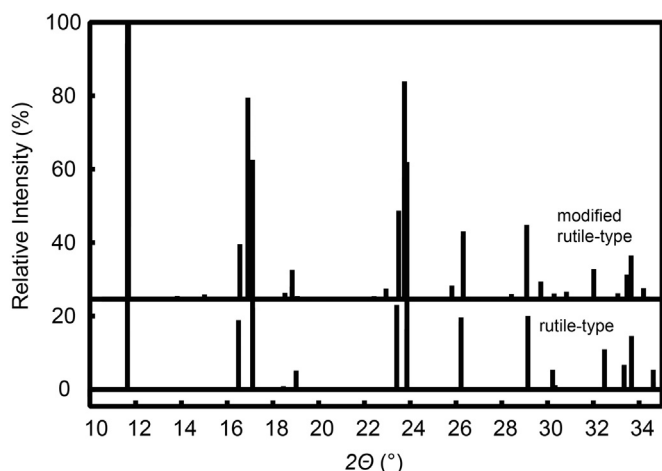
**Fig. 5.** Calculated XRD pattern (Mo radiation) of $MoO_2$ in the rutile structure (bottom) and the modified rutile structure (top).
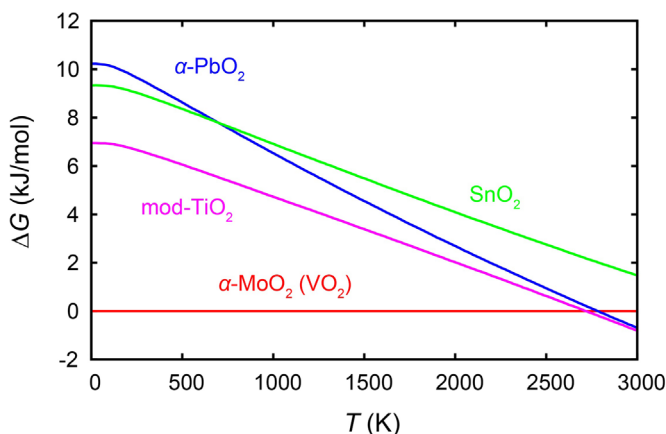


**Fig. 6.** Relative Gibbs energy versus temperature for selected $MoO_2$ structure types (VASP/PBE).

that alter along the rutile $c$ axis: 2.489 Å and 3.112 Å for $\alpha$-$MoO_2$ vs. 2.518 Å and 3.016 Å for the modified rutile type. Along the rutile $a$ axis, however, the modified structure has equivalent Mo–Mo distances while the [$VO_2$] structure shows distances of 5.052 Å and 4.712 Å.

What remains is an uncertainty concerning the two previous reports of $MoO_2$ in the rutile type. If we take the here performed calculations seriously, the experimentally proposed rutile phase of $MoO_2$ presumably represent the here reported modified rutile

type. This assumption is supported by the calculated X-ray diffraction pattern of $MoO_2$ for the rutile and modified rutile structure, as can be seen in Fig. 5. The diffraction patterns are very similar and the reflections that are split in the modified rutile structure (e.g., at 17° and 24° in 2 Θ) are so close together that a good resolution is necessary to detect the difference. We suggest that this might be the reason why Seisenbaeva et al. did not report the "modified" rutile but rutile structure instead.

Thermodynamic calculations based on the quasi-harmonic approximation provide relative Gibbs energies as a function of the temperature. Because these calculations are very time-consuming, only the four energetically lowest structures [$VO_2$], [mod-$TiO_2$], [$SnO_2(II)$] and [$\alpha$-$PbO_2$] were considered. Fig. 6 shows that the modified rutile-type [mod–$TiO_2$] becomes thermodynamically more stable than [$VO_2$] ($\alpha$-$MoO_2$) at temperatures above 2700 K. The reported synthesis by Seisenbaeva [26], however, only requires temperatures as low as 500 K to decompose the precursor and obtain the modified rutile type. The thermodynamic barrier at such low temperatures is only about 5 kJ/mol.

The [$\alpha$-$PbO_2$] phase is thermodynamically more stable than [$VO_2$]-type $\alpha$-$MoO_2$ starting at around 2700 K despite its questionable dynamic stability. According to Tamman's rule [38], typical solid-state reactions require a temperature of at least 2/3 of the melting or decomposition temperature of the most "volatile" educt. For molybdenum dioxide ($T_m = 2600$ K [39]), the resulting reaction temperature has to be at least 1750 K where the thermodynamic barrier is lower than 4 kJ/mol.

The dynamically stable [$SnO_2(II)$]-type of $MoO_2$ exhibits a small energy difference of less than 10 kJ/mol with respect to the stable $\alpha$-$MoO_2$ structure between zero and 3000 K. The literature describes two different syntheses for $SnO_2(II)$ which might also be adaptable for $MoO_2$: a synthesis at 800 °C and 158 kbar [40] and a vapor deposition at temperatures of 850 K on $\alpha$-quartz($10\bar{1}0$) [41]. Both synthetic routes employ temperatures between 850 and 1100 K where $\Delta G$ is only about 7–8 kJ/mol, small enough for an elaborate synthesis.

To investigate possible high-pressure polymorphs of $MoO_2$ the volumes of all 15 optimized structures at ambient pressure (Table 1) were varied by scaling the cell parameters between 94% and 104%. The resulting energy vs. volume data were fitted to the Birch–Murnaghan equation of state and, by doing so, the energy as a function of the pressure was obtained. The enthalpy results via $H = E + pV$. In Fig. 7 (left) the pressure-dependent relative enthalpy, $\Delta H$, of potential high-pressure polymorphs is depicted relative to the stable $\alpha$-$MoO_2$ [$VO_2$] phase. As the calculated enthalpy is only valid within the calculated volume regime, enthalpies for even smaller volumes were extrapolated for the remaining part of the energy vs. volume plot, that is, up to 100 GPa (dashed lines in Fig. 7). Although many of the investigated structures show smaller volumes than the
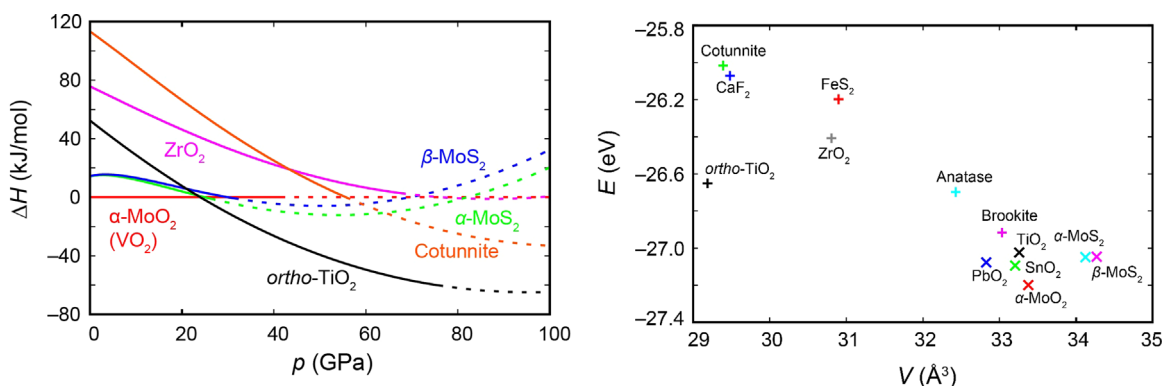


**Fig. 7.** Relative enthalpy of potential high-pressure polymorphs of $MoO_2$ compared to $\alpha$-$MoO_2$ (left). Dashed lines have been extrapolated. All other investigated polymorphs display a larger enthalpy than $\alpha$-$MoO_2$ over the entire pressure region. The energy versus volume of all investigated structure types is depicted in the right graph.

stable $\alpha$-MoO$_2$ phase upon structural relaxation (Fig. 4, right) and are therefore possible high-pressure candidates, only a few structure types attain a lower enthalpy than $\alpha$-MoO$_2$ up to 100 GPa. Surprisingly, the two [MoS$_2$] structure types seem to be slightly favored over $\alpha$-MoO$_2$ between 25 and 75 GPa although both show a larger volume at ambient pressure than $\alpha$-MoO$_2$. This unusual behavior is due to the layered nature of the crystal structure.

Previous studies [42,43] on high-pressure polymorphs of TiO$_2$ indicated that all titaniumgroup dioxides (TiO$_2$, ZrO$_2$, HfO$_2$) follow the same path under compression at ambient temperature, namely rutile→$\alpha$–PbO$_2$→baddeleyite (ZrO$_2$)→orthorhombic OI (*Pbca*) structure→cotunnite (OII). Although MoO$_2$ crystallizes in the rutile-related structure [VO$_2$], it does not follow the same path under pressure. In fact, the rutile and the $\alpha$-PbO$_2$ types display a larger enthalpy than [VO$_2$] over the entire pressure region. The enthalpy of the baddeleyite-type [ZrO$_2$] is only slightly lower at pressures around 80 GPa. As Fig. 7 shows, the clear candidates for a high-pressure polymorph of MoO$_2$ are the orthorhombic [*ortho*-TiO$_2$] structure type (OI) and the [cotunnite] type (OII). The calculations yield a pressure-induced phase transition from $\alpha$-MoO$_2$ [VO$_2$] to the orthorhombic [*ortho*-TiO$_2$] structure type at about 25 GPa. A further pressure-induced transformation to the [cotunnite] type up to 100 GPa is impossible as the cotunnite phase always displays a larger enthalpy than the [*ortho*-TiO$_2$] phase. For the same reason, neither $\alpha$-MoS$_2$ nor $\beta$-MoS$_2$ are high-pressure phases of MoO$_2$ according to our calculations.

The orthorhombic [*ortho*-TiO$_2$] structure type was first observed in a high-pressure study of TiO$_2$ [42]. It crystallizes in the orthorhombic space group *Pbca* (No. 60) and is closely related to brookite crystallizing in the same space group. While brookite is made from distorted octahedra with a sixfold coordination of the central metal atom, the [*ortho*-TiO$_2$] structure is distorted in such a way that the coordination sphere of the metal atoms is sevenfold, in harmony with the pressure–coordination number rule.

Phonon calculations have been performed to investigate the dynamic stability of the polymorphs showing lower enthalpies under pressure than $\alpha$-MoO$_2$ [VO$_2$]. The phonon density-of-states (pDOS) of [*ortho*-TiO$_2$] has been calculated for various pressures and is shown in Fig. 8 both for ambient pressure and at the approximate transition pressure of about 25 GPa. At both pressures no imaginary modes are visible, thus indicating a stable high-pressure polymorph of MoO$_2$ in the orthorhombic [*ortho*-TiO$_2$] structure.

An analogous investigation was performed for the other possible high-pressure phases. While the calculated phonon DOS of $\alpha$-MoS$_2$ and $\beta$-MoS$_2$ confirmed their dynamic stability at ambient pressure, both phases develop imaginary modes at their respective transition pressures and are thus unstable. The cotunnite phase exhibits imaginary modes already at ambient pressure and is therefore unsuitable as a high-pressure polymorph. This clearly suggests that the orthorhombic [*ortho*-TiO$_2$] structure is the only possible high-pressure polymorph of MoO$_2$ within the investigated pressure range, and it should form at around 25 GPa.

## 4. Conclusion

The system MoO$_2$ has been investigated using density-functional theory. The objective of this investigation was to find (metastable) polymorphs of MoO$_2$ that are accessible via temperature-induced reactions or through high-pressure syntheses.

Judging from the electronic energies three polymorphs are the most promising: a modified rutile structure [mod-TiO$_2$], the [$\alpha$-PbO$_2$] structure and the [SnO$_2$(II)] type which are all only about 0.1 eV less stable than the experimental $\alpha$-MoO$_2$ [VO$_2$]. The modified rutile structure evolves from the rutile-type as the dynamically stable modification while thermodynamic calculations show an energy difference of less than 7 kJ/mol. The calculated X-ray diffraction pattern is very similar to that of the non-modified rutile structure and it seems likely that the experimentally reported rutile-type MoO$_2$ is, in fact, the here proposed modified rutile structure. Phonon calculations of the [SnO$_2$(II)] structure verified the dynamic stability, and the thermodynamic calculations reveal an energy difference to the stable [VO$_2$] structure of less than 10 kJ/mol. At a proposed synthetic temperature of about 1100 K, $\Delta G$ is only about 7 kJ/mol such that a synthesis of MoO$_2$ in the [SnO$_2$(II)] structure should be possible, given a clever route. The calculated phonon DOS of [$\alpha$-PbO$_2$] reveals a small amount of imaginary modes such that the dynamic stability of the phase could not be confirmed without doubt. An attempt to modify the structure by shifting the atoms along the eigenvectors of the imaginary modes to gain a stable structure did not succeed. Thermodynamic calculations show that this structure, although dynamically unstable, becomes favorable over [VO$_2$] at temperatures larger than 2700 K, and the energy difference is smaller than 4 kJ/mol for temperatures above 1750 K, a temperature one would expect according to Tamman's rule. Although [$\alpha$-PbO$_2$] is dynamically unstable, a synthesis might still be tried as was recently successfully shown for the similarly unstable $\gamma$-TaON [35,37].

The high-pressure behavior of MoO$_2$ was investigated using quantum-chemical calculations with varying pressure. Among all
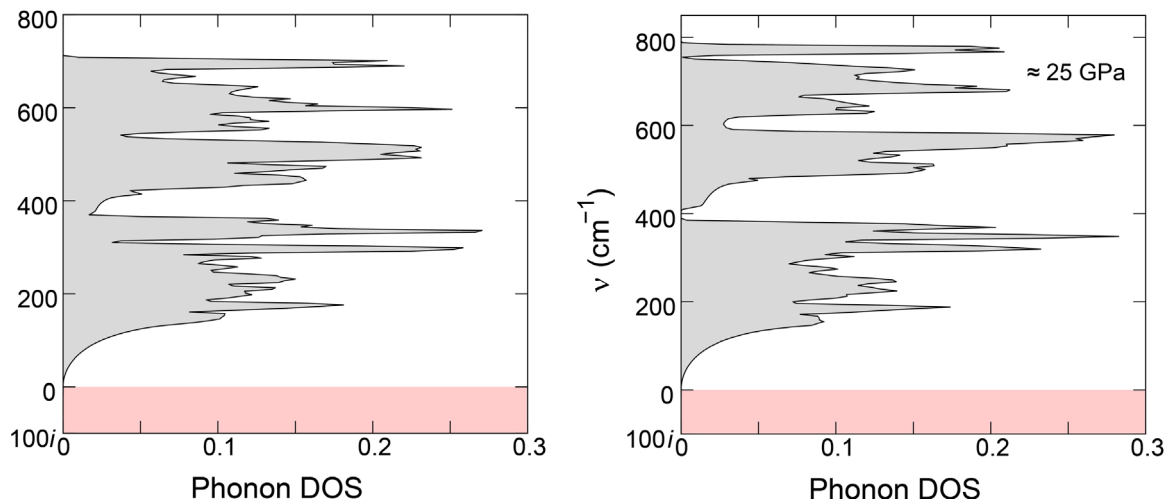


**Fig. 8.** Calculated phonon density of states of the orthorhombic [*ortho*-TiO$_2$] phase of MoO$_2$ at ambient pressure (left) and at the transition pressure of about 25 GPa.

the investigated structures with a smaller volume than the experimentally observed $\alpha$-MoO$_2$ [VO$_2$] structure, only the [*ortho*-TiO$_2$] structure is suitable as a high-pressure polymorph and should be obtained at pressures above 25 GPa.

## Acknowledgement

## Appendix A. Supporting information

Supplementary data associated with this article can be found in the online version at http://dx.doi.org/10.1016/j.jssc.2016.03.002.

## References

[1] A.F. Hollemann, N. Wiberg, Lehrbuch der Anorganischen Chemie, 34 ed., de Gruyter, Berlin, 1995.
[2] B.G. Brandt, A.C. Skapski, Acta Chem. Scand. 21 (1967) 661–672.
[3] M.A. Camacho-López, L. Escobar-Alarcón, M. Picquart, R. Arroyo, G. Córdoba, E. Haro-Poniatowski, Opt. Mater. 33 (2011) 480–484.
[4] Y. Shi, B. Guo, S.A. Corr, Q. Shi, Y.-S. Hu, K.R. Heier, L. Chen, R. Seshadri, G. D. Stucky, Nano Lett. 9 (2009) 4215–4220.
[5] A. Katrib, J.W. Sobczak, M. Krawczyk, L. Zommer, A. Benadda, A. Jablonski, G. Maire, Surf. Interface Anal. 34 (2002) 225–229.
[6] A. Katrib, D. Mey, G. Maire, Catal. Today 65 (2001) 179–183.
[7] O. Marin-Flores, L. Scudiero, S. Ha, Surf. Sci. 603 (2009) 2327–2332.
[8] A. Katrib, P. Leflaive, L. Hilaire, G. Maire, Catal. Lett. 38 (1996) 95–99.
[9] Y. Liang, S. Yang, Z. Yi, X. Lei, J. Sun, Y. Zhou, Mat. Sci. Eng. B 121 (2005) 152–155.
[10] L.C. Yang, Q.S. Gao, Y. Tang, Y.P. Wu, R. Holze, J. Power Sources 179 (2008) 357–360.
[11] Y. Sun, X. Hu, W. Luo, Y. Huang, ACS Nano 5 (2011) 7100–7107.
[12] M. Winter, J.O. Besenhard, M.E. Spahr, P. Novák, Adv. Mater. 10 (1998) 725–763.
[13] Y. Liang, Z. Yi, S. Yang, L. Zhou, J. Sun, Y. Zhou, Solid State Ion. 177 (2006) 501–505.
[14] Y.-R. Ma, C.-C. Tsai, S.F. Lee, K.-W. Cheng, Y. Liou, Y.D. Yao, J. Magn. Magn. Mater. 304 (2006) e13–e15.
[15] X. Liu, Y. He, S. Wang, Q. Zhang, J. Alloy Compd. 509 (Suppl 1) (2011) S408–S411.
[16] G.E. Buono-Core, G. Cabello, A.H. Klahn, A. Lucero, M.V. Nuñez, B. Torrejón, C. Castillo, Polyhedron 29 (2010) 1551–1554.
[17] B. Hu, L. Mai, W. Chen, F. Yang, ACS Nano 3 (2009) 478–482.
[18] D.B. Rogers, R.D. Shannon, A.W. Sleight, J.L. Gillson, Inorg. Chem. 8 (1969) 841–849.
[19] T.A. Sasaki, T. Soga, H. Adachi, Phys. Status Solidi B 113 (1982) 647–655.
[20] J.K. Burdett, Inorg. Chem. 24 (1985) 2244–2253.
[21] H. Yoshino, K. Shimokoshi, E. Miyazaki, J. Electron. Spectrosc. Relat. Phenom. 36 (1985) 269–279.
[22] T.A. Sasaki, K. Kiuchi, Chem. Phys. Lett. 84 (1981) 356–360.
[23] V. Eyert, R. Horny, K.H. Höck, S. Horn, J. Phys. Condens. Mater. 12 (2000) 4923.
[24] D.O. Scanlon, G.W. Watson, D.J. Payne, G.R. Atkinson, R.G. Egdell, D.S.L. Law, J. Phys. Chem. C. 114 (2010) 4636–4645.
[25] V.M. Goldschmidt, T. Barth, D. Holmsen, G. Lunde, W. Zachariasen, Skrifter utgitt av det Norske Videnskaps-Akademi i Oslo 1: Matematisk-Naturvidenskapelig Klasse, Vol. 1, 1926, p. 21.
[26] G.A. Seisenbaeva, M. Sundberg, M. Nygren, L. Dubrovinsky, V.G. Kessler, Mater. Chem. Phys. 87 (2004) 142–148.
[27] G. Kresse, J. Furthmüller, Comput. Mater. Sci. 6 (1996) 15–50.
[28] P.E. Blöchl, Phys. Rev. B 50 (1994) 17953–17979.
[29] J.P. Perdew, K. Burke, M. Ernzerhof, Phys. Rev. Lett. 78 (1997) 1396.
[30] J.P. Perdew, K. Burke, M. Ernzerhof, Phys. Rev. Lett. 77 (1996) 3865–3868.
[31] S. Grimme, J. Antony, S. Ehrlich, H. Krieg, J. Chem. Phys. 132 (2010) 154104.
[32] S. Grimme, S. Ehrlich, L. Goerigk, J. Comput. Chem. 32 (2011) 1456–1465.
[33] F. Birch, Phys. Rev. 71 (1947) 809–824.
[34] A. Togo, F. Oba, I. Tanaka, Phys. Rev. B 78 (2008) 134106.
[35] R.P. Stoffel, C. Wessel, M.-W. Lumey, R. Dronskowski, Angew. Chem. Int. Ed. 49 (2010) 5242–5266.
[36] E. Muller, Acta Crystallogr. B 40 (1984) 359–363.
[37] H. Schilling, A. Stork, E. Irran, H. Wolff, T. Bredow, R. Dronskowski, M. Lerch, Angew. Chem. Int. Ed. 46 (2007) 2931–2934.
[38] G. Tammann, Lehrbuch der Metallkunde, 4 ed., Verlag Voss, Berlin, 1929.
[39] B. Predel, In: O. Madelung (Ed.), Landolt-Börnstein-Group IV Physical Chemistry, Springer, Berlin, 1997, p. 1.
[40] K. Suito, N. Kawai, Y. Masuda, Mat. Res. Bull. 10 (1975) 677–680.
[41] K. Bräuer, K. Meyer, B. Müller, E. Müller, Krist. Tech. 16 (1981) 53–58.
[42] N.A. Dubrovinskaia, L.S. Dubrovinsky, R. Ahuja, V.B. Prokopenko, V. Dmitriev, H.P. Weber, J.M. Osorio-Guillen, B. Johansson, Phys. Rev. Lett. 87 (2001).
[43] Z. Fu, Y. Liang, S. Wang, Z. Zhong, Phys. Status Solidi B 250 (2013) 2206–2214.
[44] R. Blachnik, D'Ans Lax Taschenbuch für Chemiker und Physiker, 4 ed., Springer, Berlin, 1998.
[45] E.P. Meagher, G.A. Lager, Can. Mineral. 17 (1979) 77–85.
[46] F. Théobald, R. Cabala, J. Bernard, J. Solid State Chem. 17 (1976) 431–438.
[47] D.K. Smith, W. Newkirk, Acta Crystallogr. 18 (1965) 983–991.
[48] H.M. Parker, W.J. Whitehouse, Philos. Mag. 14 (1932) 939–961.
[49] L.S. Dubrovinsky, N.A. Dubrovinskaia, V. Swamy, J. Muscat, N.M. Harrison, R. Ahuja, B. Holm, B. Johansson, Nature 410 (2001) 653–654.